Journal of Vacuum Science & Technology B

Influence of N 2 O plasma treatment on microstructure and thermal stability of WN x barriers for Cu interconnection

Kou-Chiang Tsai, Wen-Fa Wu, Jen-Chung Chen, Te-Jen Pan, and Chuen-Guang Chao

Citation: Journal of Vacuum Science & Technology B **22**, 993 (2004); doi: 10.1116/1.1715087
View online: http://dx.doi.org/10.1116/1.1715087
View Table of Contents: http://scitation.aip.org/content/avs/journal/jvstb/22/3?ver=pdfcov
Published by the AVS: Science & Technology of Materials, Interfaces, and Processing

Articles you may be interested in

Deposition of W N x C y for diffusion barrier application using the imido guanidinato complex W (N i Pr) Cl 3 [Pr i N C (N Me 2) N i Pr]
J. Vac. Sci. Technol. B **26**, 1800 (2008); 10.1116/1.2981082

W 2 B and Cr B 2 diffusion barriers for Ni Au contacts to p - Ga N
Appl. Phys. Lett. **91**, 042105 (2007); 10.1063/1.2762280

Evaluation of integrity and barrier performance of atomic layer deposited W N x C y films on plasma enhanced chemical vapor deposited Si O 2 for Cu metallization
Appl. Phys. Lett. **89**, 081913 (2006); 10.1063/1.2338768

Effects of N H 3 pulse plasma on atomic layer deposition of tungsten nitride diffusion barrier
J. Vac. Sci. Technol. B **24**, 1432 (2006); 10.1116/1.2203639

Low leakage current Cu(Ti)/SiO 2 interconnection scheme with a self-formed TiO x diffusion barrier
Appl. Phys. Lett. **80**, 2678 (2002); 10.1063/1.1468913

Re-register for Table of Content Alerts

Create a profile.

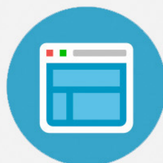

Sign up today!

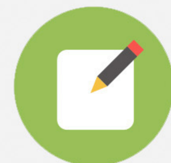

Redistribution subject to AVS license or copyright; see http://scitation.aip.org/termsconditions. Download to IP: 140.113.38.11 On: Thu, 01 May 2014 04:25:29

Influence of N_2O plasma treatment on microstructure and thermal stability of WN_x barriers for Cu interconnection

Kou-Chiang Tsai
Department of Materials Science and Engineering, National Chiao Tung University, Hsinchu 300, Taiwan, Republic of China

Wen-Fa Wu[a]
National Nano Device Laboratories, Hsinchu 300, Taiwan, Republic of China

Jen-Chung Chen, Te-Jen Pan, and Chuen-Guang Chao
Department of Materials Science and Engineering, National Chiao Tung University, Hsinchu 300, Taiwan, Republic of China

(Received 13 August 2003; accepted 1 March 2004; published 4 May 2004)

Thermal stabilities of Cu-contacted n^+-p junctions with tungsten nitride (WN_x) diffusion barriers deposited at various nitrogen flow ratios are investigated. N_2O plasma treatment is applied to improve thermal stability and barrier performance of WN_x film. Sheet resistance of Cu/N_2O plasma-treated WN_x/Si is fairly stable even after annealing at 750 °C for 30 min. Moreover, N_2O plasma treatment enables the Cu/WN_x/n^+-p junction diodes to sustain thermal annealing at 600 °C without electrical degradation. Auger electron spectroscopy depth profiles show that Cu diffusion through the N_2O plasma-treated WN_x barrier is extremely limited, even after annealing at 675 °C. Analyses of transmission electron microscopy and x-ray photoemission spectroscopy show that nitridation and oxidation on the WN_x barrier occur and an amorphous layer is formed after N_2O plasma treatment. © *2004 American Vacuum Society.* [DOI: 10.1116/1.1715087]

I. INTRODUCTION

In microelectronic devices, the critical feature sizes of integrated circuits have been greatly reduced to improve packing density. Cu has been used as an on-chip interconnection in microelectronic devices recently due to its lower electrical resistivity and better electromigration resistance compared to aluminum.[1,2] However, for the application of Cu metallization, the interaction between Si and Cu is very severe and will degrade electrical performance of the device even at temperatures as low as 200 °C.[3,4] A barrier layer is needed to prevent the copper diffusion. Refractory metals and their nitrides had been investigated for such application. Among several metal nitrides, tungsten nitride (WN_x) is a commonly used material in integrated-circuit technologies because of its refractory nature and high thermal stability.[5,6] Furthermore, tungsten nitride is promising compared to tantalum or other barriers due to excellent chemical mechanical polishing process compatibility.[7] However, the dominant failure of the sputtered WN_x barrier is attributed to diffusion via fast diffusion paths in grain boundaries.[8,9] Copper and silicon interdiffuse through the grain boundaries of the WN_x barrier during annealing at an elevated temperature, resulting in degraded electrical characteristics, and ultimately, in device failure.

One method used to retard Cu penetration involves intentionally contaminating the barrier with either nitrogen or oxygen. Theoretically, these impurities would physically block the fast diffusion paths, or chemically react with Cu to enhance the barrier properties. Another method to avoid fast diffusion paths along grain boundaries is to change the microstructure of the barrier from a crystalline to an amorphous structure.[10–13] In this research, reactively sputtered WN_x barriers were used as the diffusion barriers for Cu metallization. The effects of nitrogen flow ratio during sputtering were investigated. Barrier performance of the WN_x layer can be improved by changing microstructure and stuffing grain boundaries with N_2O plasma treatment. We found that N_2O plasma treatment exhibits nitridation and oxidation of the WN_x barrier and results in an amorphous surface layer. But this treatment also stuffs nitrogen and oxygen atoms into grain boundaries of WN_x barriers.

II. EXPERIMENT

Single-crystal, (100)-orientated silicon wafers were used in this study. WN_x films were deposited onto Si substrates by reactive sputtering of the W target after the substrates were cleaned in a dilute HF solution. The sputtering chamber was evacuated to a pressure less than 6×10^{-7} Torr, and sputtering pressure was 6×10^{-3} Torr during deposition. Deposition was carried out at room temperature without intentional heating. WN_x films of 50 nm thickness were sputtered at a direct current power of 1000 W under nitrogen flow ratio $N_2/(Ar+N_2)$ of 10%, 15%, 20%, or 30%. Some WN_x films received N_2O plasma post-treatments in a plasma-enhanced chemical vapor deposition (PECVD) system. The power and pressure were 200 W and 100 mTorr, respectively, for N_2O plasma post-treatment. For easy identification, the WN_x film sputtered at a nitrogen flow ratio of $a\%$ and N_2O plasma-treated WN_x film were denoted as $WN_x(a\%)$ and $WN_x(N_2O)$, respectively, in the work. Subsequently, the Cu

[a]Author to whom correspondence should be addressed; electronic mail: wfwu@ndl.gov.tw

Redistribution subject to AVS license or copyright; see http://scitation.aip.org/termsconditions. Download to IP: 140.113.38.11 On: Thu, 01 May 2014 04:25:29

TABLE I. Properties of tungsten nitride barriers deposited at various nitrogen flow ratios used in the study.

	$N_2/(Ar+N_2)=10\%$	15%	20%	30%
Deposition rate (Å/min)	177.6	163.5	160.8	153.2
Resistivity ($\mu\Omega$ cm)	148.5	168.2	172.5	200.1
Stress (dyne/cm^2)	1.55×10^{-10}	1.45×10^{-10}	1.43×10^{-10}	1.40×10^{-10}
Root-mean-square roughness (nm)	2.05	0.56	0.31	0.28
Grain size (nm) measured from TEM	10–20	8–15	5–13	<10
Atomic ratio (W/N) measured from RBS	0.75/0.25	0.67/0.33	0.64/0.36	0.62/0.38
Density (g/cm^3) measured from RBS	17.39	17.07	16.9	16.33

film with thickness of 300 nm was sputtered onto the WN_x barrier. The Cu/WN_x/Si samples were annealed at 550–750 °C in N_2 ambient for 30 min to investigate thermal stability.

Film thickness was measured by a stylus surface profiler and scanning electron microscopy. Transmission electron microscopy (TEM) and x-ray diffraction (XRD) were used to determine microstructure and crystalline orientation of the film. Rutherford backscattering spectroscopy (RBS) was used to determine the composition and density of the WN_x film. X-ray photoemission spectroscopy (XPS) was used to study the bonding structures and chemical binding energies. A four-point probe system was employed to measure sheet resistance. Compositional depth profiles after annealing were analyzed by Auger electron microscopy (AES).

The failure of the WN_x barrier between Cu and Si was determined by leakage current of the n^+-p junction diode. The local oxidation of silicon process was applied to the wafer to define active regions after cleaning. The n^+-p junctions were formed by As^+ implantation at 60 keV with a dose of 5×10^{15} cm^{-2}, followed by rapid thermal annealing at 1050 °C for 30 s in N_2 ambient. The WN_x film was etched using $CF_4/CHF_3/O_2$ plasma after copper patterns were etched by a diluted HNO_3 solution. Leakage currents of the diodes were measured at a reverse bias of 5 V by a HP4145B semiconductor parameter analyzer after annealing at various temperatures for 30 min.

III. RESULTS AND DISCUSSION

Table I is the summary of properties of WN_x barriers sputtered at various nitrogen flow ratios. The nitrogen concentration of WN_x film increases as the nitrogen flow ratio increases from 10% to 30%. The corresponding nitrogen content of WN_x films increases from 25 to 38 at. % from RBS analyses. The deposition rate of WN_x film decreases with increasing nitrogen flow ratio. The decreasing deposition rate at a high nitrogen flow ratio is attributed to the sputtering yield of nitrogen being lower than that of argon. The effective sputtering yield decreases with decreasing argon flow ratio, and hence, the deposition rate decreases, as listed in Table I. Figure 1 displays a cross-sectional TEM image of a reactively sputtered WN_x(20%) film. Columnar grains are observed, as shown in Fig. 1. The columns may develop via a surface diffusion process influenced by both geometrical shadowing effects and limited atomic mobility.[14,15] The grain size of sputtered WN_x film decreases with increasing nitrogen content, as indicated in Table I. The decreasing grain size can be explained in terms of nitrogen enrichment at the grain surface, which prevents further growth, and hence, contributes to finer grains and the decrease of surface roughness, as shown in Table I. Moreover, as the nitrogen flow ratio increases, the resistivity increases because numerous of disorder regions and vacancies occur among the WN_x grains and grain boundaries. Furthermore, it is reported that impurities (nitrogen or oxygen) in the films are responsible for the intrinsic compressive stress.[16] In the study, a decrease of tensile stress is observed as the nitrogen concentration of WN_x film increases.

Figure 2(a) displays the variation percentage in sheet resistance of the Cu/WN_x/Si sample after furnace annealing at various temperatures. The variation percentage in sheet resistance is defined as the ratio of $(R\text{-}R_0)$ to R_0, in which R_0 and R denote the sheet resistance of as-deposited and annealed samples, respectively. The results reflect the interactions between Cu and Si indirectly. The sheet resistance initially decreases gradually with increasing annealing temperature due to the reduction of crystal defects and grain growth of the Cu film. But sheet resistance increases at a certain temperature because of failure of the diffusion layer, which results in the reaction of Cu or WN_x barrier with the

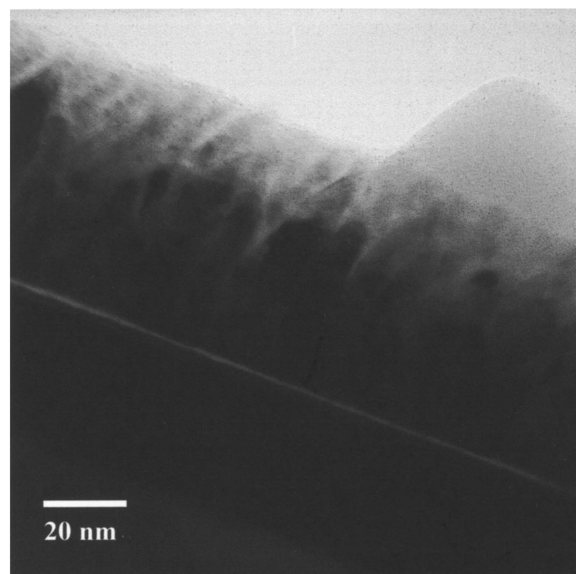

FIG. 1. Cross-sectional TEM image of the WN_x(20%) film on the Si substrate.

Redistribution subject to AVS license or copyright; see http://scitation.aip.org/termsconditions. Download to IP: 140.113.38.11 On: Thu, 01 May 2014 04:25:29

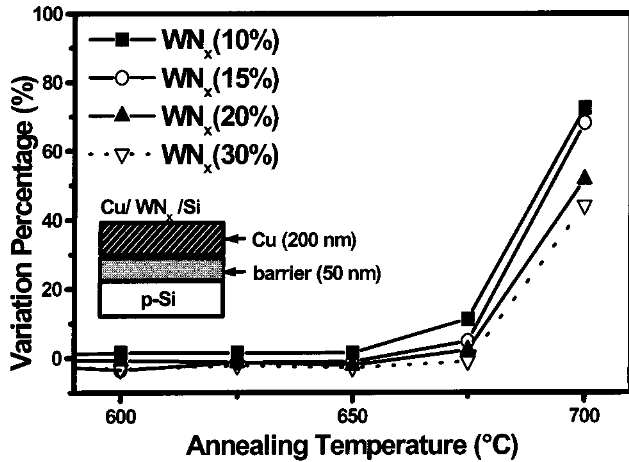

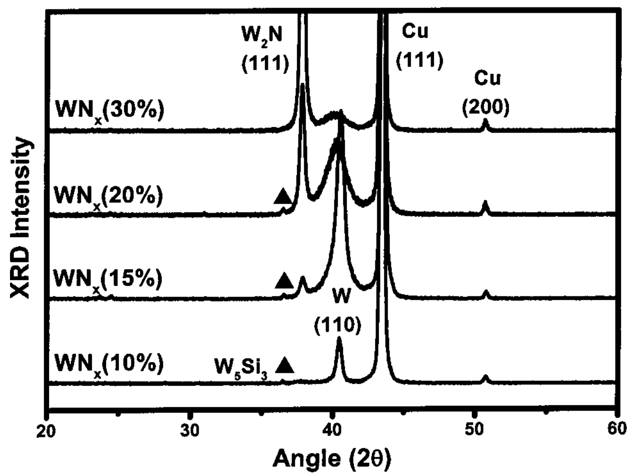

FIG. 2. (a) Variation percentage in sheet resistance of Cu/WN_x/Si contact system as a function of annealing temperature. (b) XRD spectra of Cu/WN_x/Si contact systems after annealing at 675 °C for 30 min.

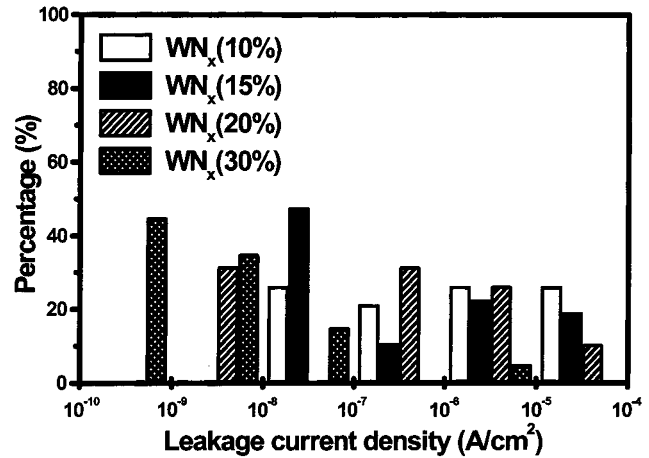

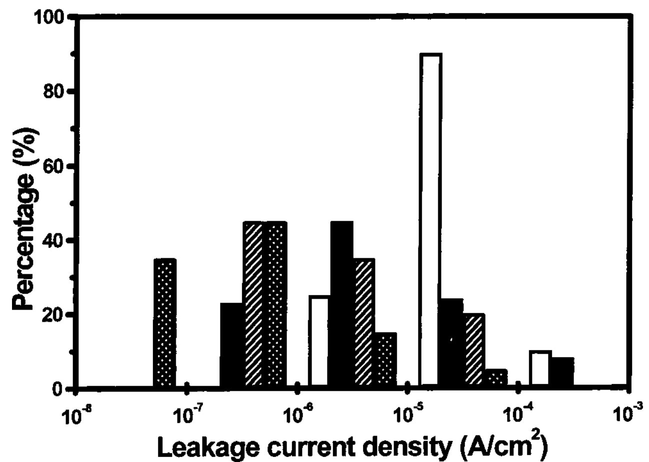

FIG. 3. Statistical distributions of leakage current densities of Cu/WN_x/n^+-p junction diodes after annealing at (a) 500 and (b) 600 °C for 30 min.

silicon substrate and formation of compounds. Figure 2(b) shows XRD patterns of the samples with the WN_x barriers deposited at various nitrogen flow ratios after annealing at 675 °C for 30 min. From XRD analyses, no compound is found for the Cu/WN_x(30%)/Si system after annealing at 675 °C. In contrast, an inferior barrier performance is observed for the WN_x barrier deposited at a lower nitrogen flow ratio because sheet resistance starts to increase and W_5Si_3 compounds are found. In addition, the nanostructured W_2N (111) and body-centered-cubic (bcc) W (100) grains are observed in nitrogen-rich WN_x(20% – 30%) barriers. It is reported that WN_x films transferred into a two-phase mixture of W and W_2N between 600 and 700 °C, and the mixture of W and W_2N plays an important role in preventing Cu diffusion even after crystallization.[17] Figure 2(b) also shows that the peak of the bcc W (100) reflection line in WN_x(10%) film is very sharp compared to that in WN_x(30%) film, and the peak of W_2N (111) is not observed. The partially incorporated nitrogen will release from the WN_x(10%) barrier during annealing at high temperature, and hence, the nitrogen-stuffing effects in the WN_x grain are eliminated, and coarse bcc W grains develop in the nitrogen-deficient WN_x(10%) barrier.

Figures 3(a) and 3(b) illustrate the statistical distributions of leakage current densities measured at a reverse bias of 5 V for the Cu/WN_x/n^+-p junction diodes annealed at 500 and 600 °C, and at least 30 diodes are measured in each case. The leakage current densities of all the samples are below 1.0×10^{-8} A/cm^2 before annealing. Almost all Cu/WN_x(30%)/n^+-p junction diodes retain low leakage current densities after annealing at 500 °C for 30 min. Furthermore, the leakage current densities are less than 10^{-7} A/cm^2 for most junction diodes with the WN_x(30%) barriers after annealing at 600 °C for 30 min. In contrast, high leakage current densities above 10^{-7} A/cm^2 are found for diodes with low-nitrogen-incorporated WN_x barriers after annealing at 600 °C. Although WN_x and Cu do not form compounds, the diffusion of a small amount of copper through the grain boundaries or defects in the WN_x barriers into the Si junction region may cause the severe failure of the shallow junction. As shown in XRD results of Fig. 2(b),

Redistribution subject to AVS license or copyright; see http://scitation.aip.org/termsconditions. Download to IP: 140.113.38.11 On: Thu, 01 May 2014 04:25:29

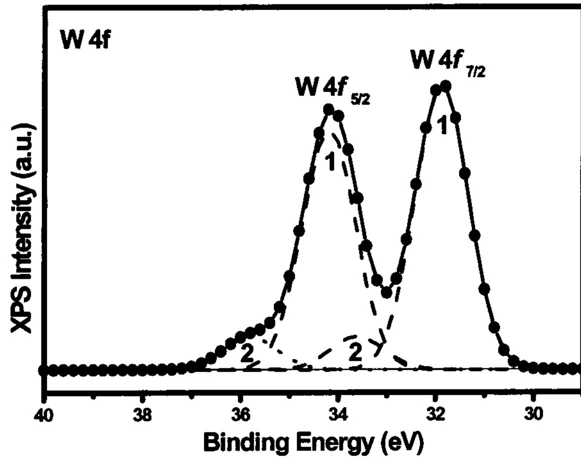

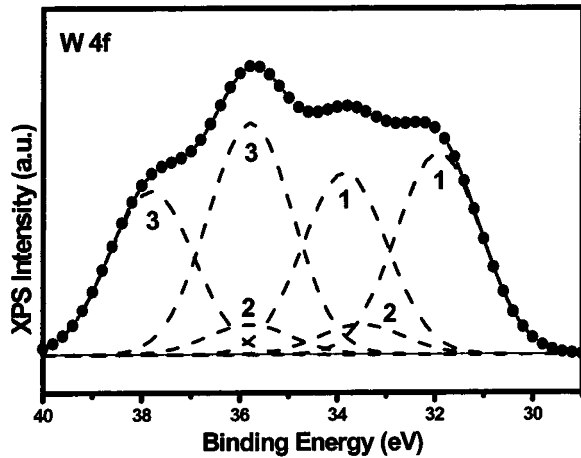

FIG. 4. XPS W 4f spectra of WN_x(15%) and $WN_x(N_2O)$ barriers.

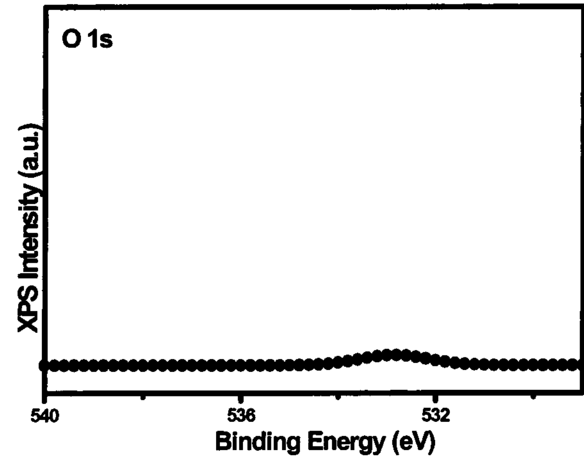

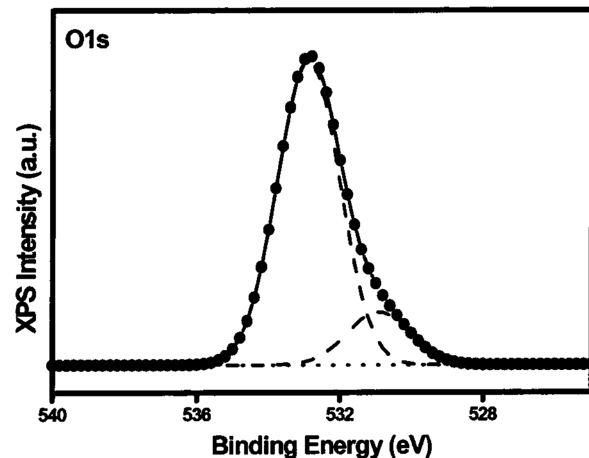

FIG. 5. XPS O 1s spectra of WN_x(15%) and $WN_x(N_2O)$ barriers.

coarse bcc W grains are formed in the WN_x(10%) barrier at 675 °C, and opened grain boundaries can significantly degrade the barrier due to formation of fast diffusion paths. On the other hand, the increasing nitrogen incorporation leads to microstructural change, which can reduce the fast diffusion paths of the barrier.

To improve the barrier effectiveness of the WN_x layer, N_2O plasma treatment is applied to treat the WN_x(15%) barrier in this work. XPS analysis was carried out to identify the chemical bonding states of barriers. Figures 4, 5, and 6 show W 4f, O 1s, and N 1s XPS spectra, respectively, of WN_x(15%) and $WN_x(N_2O)$ barriers. The W 4f peaks can be well resolved into many peaks by curve fitting, as shown in Fig. 4. Curves 1, 2, and 3 are the separated curves of the XPS superimposition spectrum. The main binding energies of the W $4f_{7/2}$ and W $4f_{5/2}$ electrons of WN_x and $WN_x(N_2O)$ barriers, resolved as curve 1 in the W 4f spectra, are 31.8 and 34.2 eV, respectively. These values are consistent with the peaks of metal tungsten.[18] The W $4f_{7/2}$ and W $4f_{5/2}$ peaks of curve 2 are 33.7 and 35.9 eV. These peaks are associated with the peaks of WN_x.[18] Two other peaks at high binding energies of 35.5 and 37.5 eV, resolved as curve 3 in Fig. 4(b), are found for the $WN_x(N_2O)$ barrier. The peaks correspond to binding energies of tungsten oxide and are attributed to oxidation during N_2O plasma treatment. There is almost no peak in the O 1s spectrum of the WN_x(15%) barrier, as shown in Fig. 5(a). However, two peaks at around 530.9 and 532.9 eV are found in the O 1s spectrum of the $WN_x(N_2O)$ barrier, as shown in Fig. 5(b). The low-energy peak at 530.9 eV corresponds to the O^{2-} ion of WO_3, and the major peak at 532.9 eV is identical to the O 1s peak of the O^{2-} ion of other combination states of WO_x.[19] This means that the oxidation occurs during N_2O plasma treatment. The major peak centered at 397 eV, as shown in the N 1s spectra of Fig. 6, is consistent with the N 1s binding energy of a nitride compound. Another peak at a higher binding energy of ~400 eV is attributed to the N atoms or molecules present in grain boundaries of WN_x.[13,20,21] The relative intensity of the peak at ~400 eV in the $WN_x(N_2O)$ barrier is much higher than that in the WN_x(15%) barrier, as shown in Fig. 6. It could be explained that most of the introduced nitrogen atoms are likely present at the grain boundaries during N_2O plasma treatment. Hence, N_2O plasma treatment enhances nitrogen

Redistribution subject to AVS license or copyright; see http://scitation.aip.org/termsconditions. Download to IP: 140.113.38.11 On: Thu, 01 May 2014 04:25:29

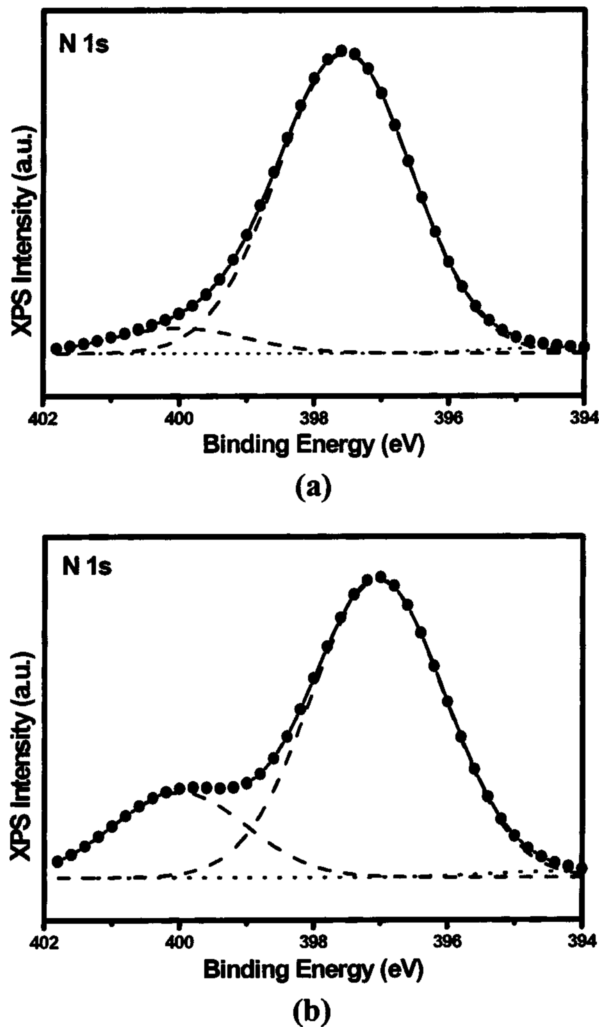

FIG. 6. XPS N 1*s* spectra of $WN_x(15\%)$ and $WN_x(N_2O)$ barriers.

atoms to stuff into the grain boundaries to block diffusion paths.

To further clarify the structure and identify possible surface reactions of the WN_x and $WN_x(N_2O)$ barriers, plan-view TEM was used to analyze the microstructure. Both the bright-field plan-view images and the selected-area diffraction (SAD) patterns of the WN_x and $WN_x(N_2O)$ barriers are shown in Fig. 7. The $WN_x(N_2O)$ barrier is composed of finer grains compared to the WN_x barrier. The SAD shows that the $WN_x(N_2O)$ barrier has clear board halos, instead of diffusion spots, indicating that the N_2O plasma treatment causes the formation of an amorphous layer on the WN_x barrier.

Figure 8(a) shows the variation percentage in sheet resistance of the Cu/barrier/Si sample after furnace annealing at various temperatures. Sheet resistance of the Cu/$WN_x(N_2O)$/Si system only increases around 20%, even after annealing at 750 °C. However, after annealing at temperatures of 600–700 °C, the sheet resistances of Cu-contacted systems with other barriers (WN_x, WC_x,[22] TiC_x,[23] physical vapor deposition TaN,[24] and CVD TaN[24]) sharply increase (⩾100%), indicating that a considerable amount of Cu has already diffused through the barrier layers

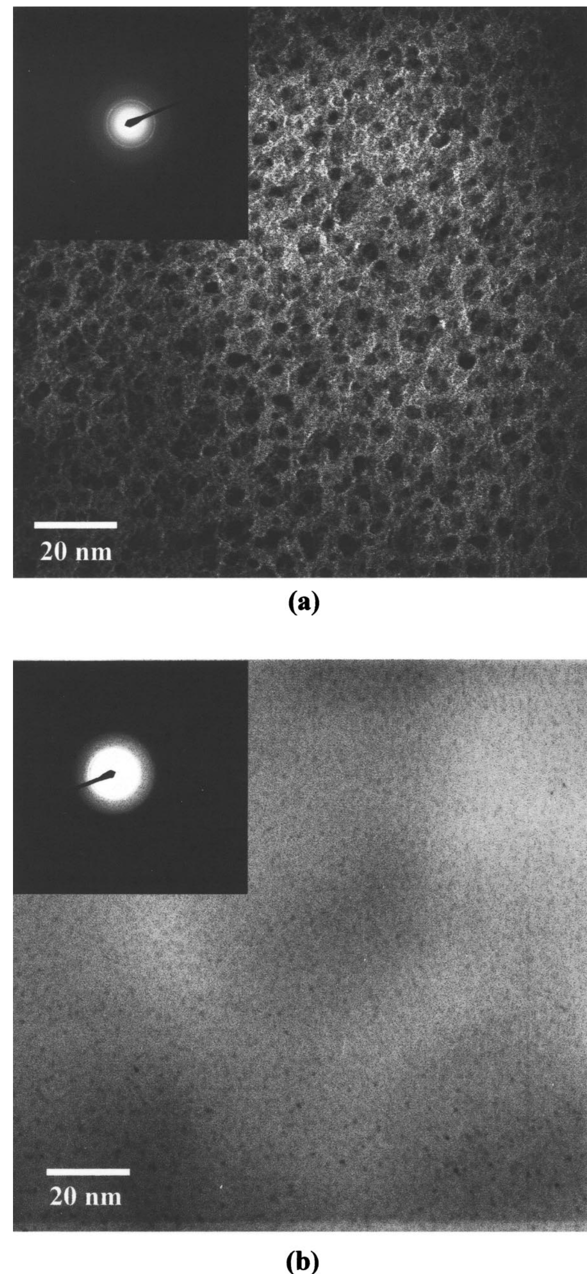

FIG. 7. Bright-field TEM images and SAD patterns of the (a) $WN_x(15\%)$ and (b) $WN_x(N_2O)$ barriers.

and reacted with Si substrates, thus resulting in Cu_3Si or barrier-Si compounds and the deterioration of the conductivity of the contact systems. Further evidence is given by XRD results, as shown in Fig. 8(b): formation of Cu_3Si compounds is observed in the Cu/WN_x/Si system after annealing at 700 °C for 30 min. Cu_3 Si compounds are not found in the system with the $WN_x(N_2O)$ barrier. According to XPS and TEM results, the nitridation and oxidation of the WN_x barrier is controlled by the mobility of the nitrogen- and oxygen-based adatoms on the WN_x surface during the N_2O plasma treatment. This can be understood by the fact that nitrogen- and oxygen-based adatoms can act as a roadblock to the

Redistribution subject to AVS license or copyright; see http://scitation.aip.org/termsconditions. Download to IP: 140.113.38.11 On: Thu, 01 May 2014 04:25:29

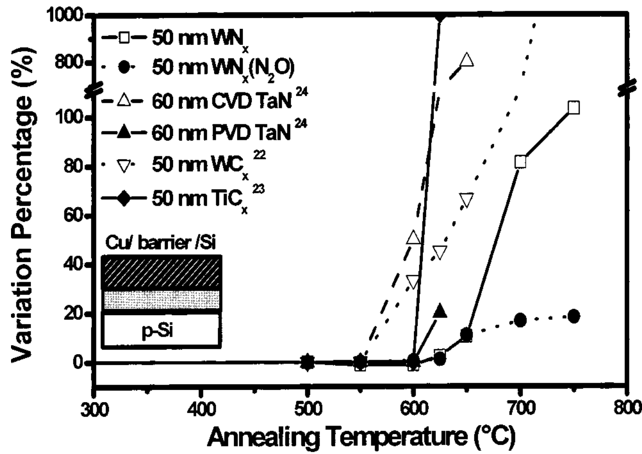

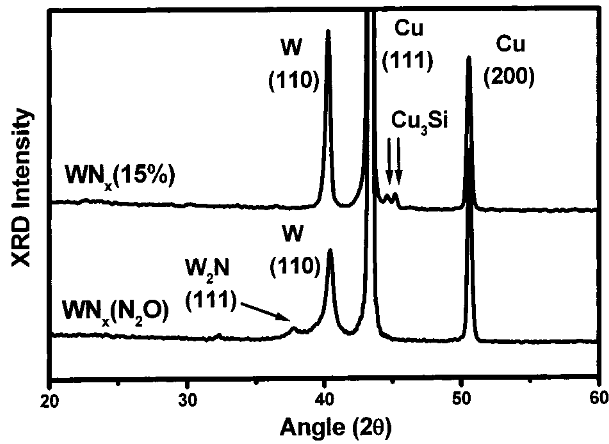

FIG. 8. (a) Variation percentage in sheet resistance of Cu/barrier/Si contact system as a function of annealing temperature. (b) XRD spectra of Cu/WN_x(15%)/Si and Cu/$WN_x(N_2O)$/Si contact systems after annealing at 700 °C for 30 min.

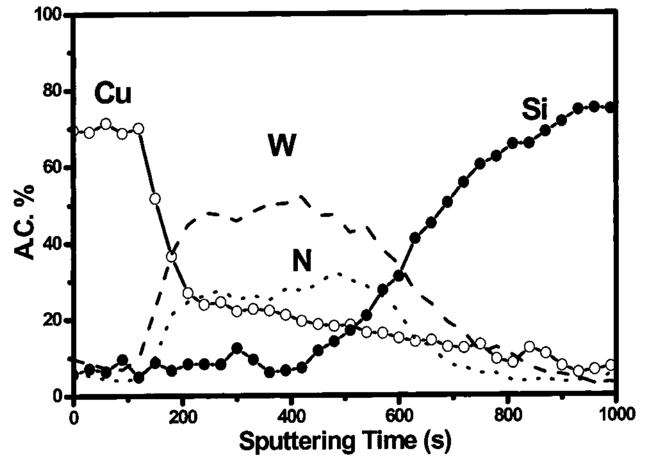

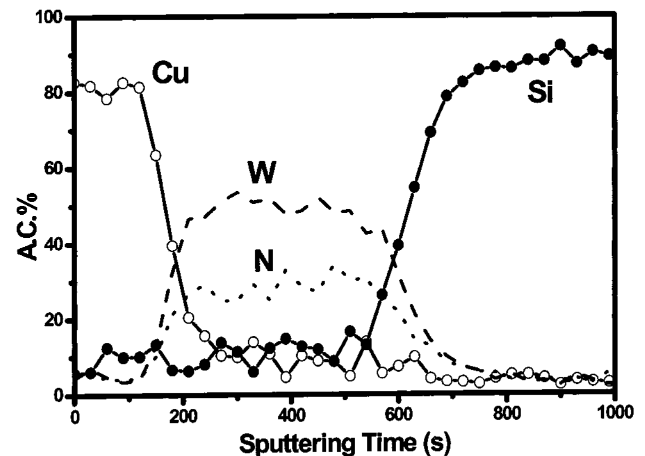

FIG. 9. AES depth profiles of Cu/WN_x(15%)/Si and Cu/$WN_x(N_2O)$/Si contact systems after annealing at 675 °C for 30 min.

WN_x or serve as nucleation sites for defects. Therefore, the WN_x grains may not have sufficient mobility to migrate to the preferred sites for crystallization growth during thermal annealing. Compared to previous research, the failure temperature (variation percentage > 50%) of the $WN_x(N_2O)$ barrier is greater than 750 °C and is superior to WC_x (~650 °C),[22] TiC_x(~625 °C),[23] and TaN(~650 °C).[24] Figure 9 displays the AES depth profiles of the Cu/WN_x/Si and Cu/$WN_x(N_2O)$/Si systems after annealing at 675 °C. Some copper diffuses through the WN_x layer into the Si substrate for the Cu/WN_x/Si system. Copper diffusion is limited, and a copper signal is not found for the Cu/$WN_x(N_2O)$/Si system.

Figures 10(a) and 10(b) indicate statistical distributions of reverse-biased leakage current densities measured at 5 V for Cu/barrier/Si junction diodes after annealing at 500 and 600 °C. The leakage current densities are less than 10^{-8} A/cm^2 before annealing. Leakage current densities of diodes with 50 nm $WN_x(N_2O)$ barriers are significantly lower than those with WN_x(50 nm), WC_x(50 nm),[22] TiC_x(50 nm),[23] or TaN(60 nm)[24] barriers after annealing at 500 °C. After 600 °C annealing, the leakage current densities of almost all diodes with WN_x, WC_x, TiC_x, or TaN barriers are higher than 10^{-7} A/cm^2. In contrast, diodes with $WN_x(N_2O)$ barriers retain low leakage current densities, and leakage current densities are less than 10^{-8} A/cm^2. It is obvious that N_2O plasma treatment will improve barrier performance effectively because it could impede Cu to diffuse into Si substrate. Effects of N_2O plasma treatment on a WN_x barrier are summarized as following. The nitrogen- and oxygen-based radicals and ions are produced in the PECVD system, and they result in nitridation and oxidation on the surface of WN_x barriers. The nitrogen atoms form covalent or ionic bonds with the tungsten to be tungsten nitrides. But excessive nitrogen atoms also stuff WN_x grain boundaries and block the rapid diffusion paths for Cu and Si atoms. On the other hand, the oxygen-based radicals or ions will react with tungsten nitride to form compounds of tungsten oxides (WO_3 and WO_x). These effects contribute to improve the effectiveness of the tungsten nitride diffusion barrier.

IV. CONCLUSION

Effects of N_2O plasma treatment on the thermal stability of the Cu/WN_x/n^+-p junction system were systematically

Redistribution subject to AVS license or copyright; see http://scitation.aip.org/termsconditions. Download to IP: 140.113.38.11 On: Thu, 01 May 2014 04:25:29

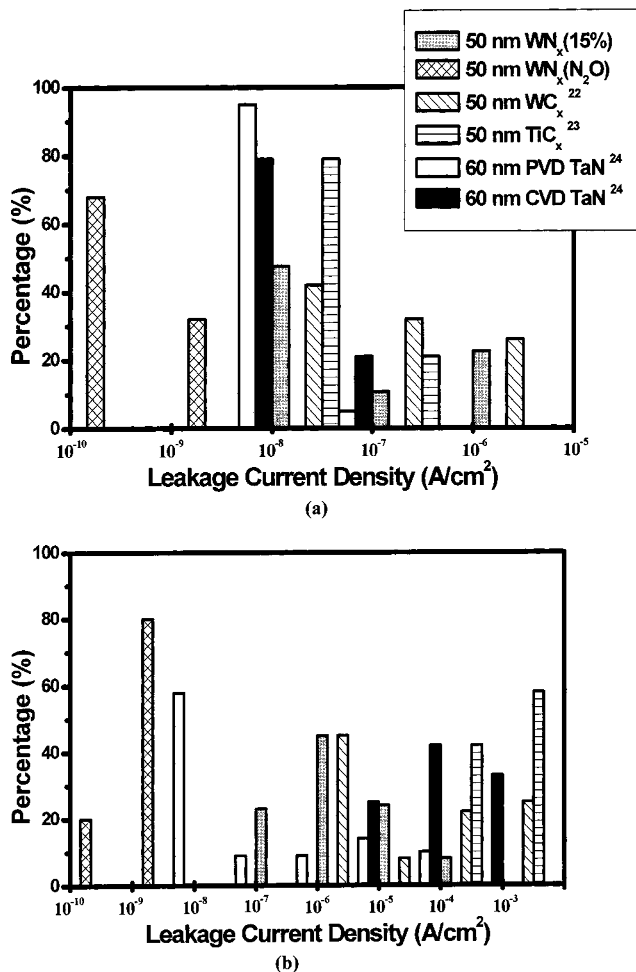

FIG. 10. Statistical distributions of leakage current densities of Cu-contacted junction diodes with various diffusion barriers after annealing at (a) 500 and (b) 600 °C for 30 min.

investigated. With N_2O plasma treatments on WN_x barriers, the $Cu/WN_x(N_2O)/Si$ systems sustained thermal annealing up to 750 °C without electrical degradation. N_2O plasma treatment resulted in nitridation and oxidation of the WN_x barrier and formation of a resulting amorphous layer on the surface. Furthermore, N_2O plasma treatment introduces excessive nitrogen atoms to stuff grain boundaries of the WN_x barrier, and hence, effectively suppresses the formation of the Cu–Si compound and improves barrier performance.

ACKNOWLEDGMENTS

The work was financially supported by the National Science Council of the Republic of China under Contract No. NSC 91-2215-E-492-002 and supported, in part, by the Ministry of Economic Affairs of the Republic of China under Contract No. 91-EC-17-A-08-S1-0003. Technical support from the National Nano Device Laboratories is greatly acknowledged.

[1]C. A. Ross, Mater. Res. Soc. Symp. Proc. **225**, 35 (1991).
[2]M. Iguchi *et al.*, *Technical Digest of the International Electron Devices Meeting* (IEEE, Washington, 1999), p. 615.
[3]J. Torres, Appl. Surf. Sci. **91**, 112 (1995).
[4]S. P. Murarka, Microelectron. Eng. **37/38**, 29 (1997).
[5]H. Li, S. Jin, H. Bender, F. Lankmans, I. Heyvaent, K. Maex, and L. Froyen, J. Vac. Sci. Technol. B **18**, 242 (2000).
[6]J. S. Becker and R. G. Gordon, Appl. Phys. Lett. **82**, 2239 (2003).
[7]S. Wong, C. Ryu, H. Lee, and K. Kwon, Mater. Res. Soc. Symp. Proc. **514**, 75 (1998).
[8]S. Ganguli, L. Chen, T. Levine, B. Zheng, and M. Chang, J. Vac. Sci. Technol. B **18**, 237 (2000).
[9]M. Hecker *et al.*, Microelectron. Eng. **64**, 269 (2002).
[10]P. J. Pokela, C. K. Kwok, E. Kowala, S. Raud, and M. A. Nicolet, Appl. Surf. Sci. **53**, 364 (1991).
[11]Y. T. Kim, C. S. Kwon, D. J. Kim, J. W. Park, and C. W. Lee, J. Vac. Sci. Technol. A **16**, 477 (1998).
[12]K. L. Ou, W. F. Wu, C. P. Chou, S. Y. Chiou, and C. C. Wu, J. Vac. Sci. Technol. B **20**, 2154 (2002).
[13]W. F. Wu, K. L. Ou, C. P. Chou, and C. C. Wu, J. Electrochem. Soc. **150**, G83 (2003).
[14]J. A. Thornton and D. W. Hoffman, Thin Solid Films **171**, 5 (1989).
[15]A. G. Dirks, R. A. M. Wolters, and A. E. M. De Veirman, Thin Solid Films **208**, 181 (1992).
[16]H. Windischmann, J. Vac. Sci. Technol. A **9**, 2459 (1991).
[17]B. S. Suh, H. K. Cho, Y. J. Lee, W. J. Lee, and C. O. Park, J. Appl. Phys. **89**, 4128 (2001).
[18]J. F. Moulder, W. F. Stickle, P. E. Sobol, and K. D. Bomben, *Handbook of X-ray Photoelectron Spectroscopy* (Physical Electronics, Eden Prairie, MN, 1995).
[19]H. L. Zhang, D. Z. Wang, and N. K. Huang, Appl. Surf. Sci. **150**, 34 (1999).
[20]T. Nakajima, K. Watanabe, and N. Watanabe, J. Electrochem. Soc. **134**, 3175 (1987).
[21]K. M. Chang, T. H. Yeh, and I. C. Deng, J. Appl. Phys. **81**, 3670 (1997).
[22]S. J. Wang, H. Y. Tsai, S. C. Sun, and M. H. Shiao, J. Electrochem. Soc. **148**, 500 (2001).
[23]S. J. Wang, H. Y. Tsai, S. C. Sun, and M. H. Shiao, J. Electrochem. Soc. **148**, 563 (2001).
[24]M. H. Tsai, S. C. Sun, C. E. Tsai, S. H. Chuang, and H. T. Chiu, J. Appl. Phys. **79**, 6932 (1996).

Redistribution subject to AVS license or copyright; see http://scitation.aip.org/termsconditions. Download to IP: 140.113.38.11 On: Thu, 01 May 2014 04:25:29